# Power system stability control and voltage stabilization for a wind farm based on adaptive dynamic programming

Ali Khodadadi[1], Mohammad Esmaeili Akbari[2], Hosein Nasir Aghdam[3]
[1,2,3]Department of Electrical Engineering, Ahar Branch, Islamic Azad University, Ahar, Iran.
Email alikhodadadi9@yahoo.com (Corresponding author)

**Abstract**

*In this research, control system based on adaptive dynamic programming (GrHDP), presented for Wind farm Double-Fed Induction Generator (DFIG) in order to improve transient stability system under error conditions. Suggersted controller, implemented according to the interaction between the controller and plant as a based- adaptive dynamic programming (ADP) and based on pproximation of optimal control mode. The programming and simulation provided in MATLAB soft ware and the effectiveness of the proposed approach corroborated via two cases: The first case investigates a revised four-machine two-area system with high wind penetration and a static synchronous compensator. The second case is a practical size power system with wind farm based on actual data. In addition, detailed simulation analysis and comparative studies with traditional ADP approaches presented to demonstrate the superior performance of our method.*

**Keywords**: Double-Fed Induction Generator (DFIG), adaptive dynamic programming (ADP), adaptive dynamic programming.

## 1. Introduction

The installed capacity for using wind energy has been increased in the world from 7600 MW to 31000 MW means that roughly 4 times since the end of 1997 to end of 2002 [1]. Large and small wind turbines have been made to provide power in the units of multi-megawatt power ability in contries inclouded Germany, Denmark, America, Spain, UK and many other countries [2-5]. Considering to the existence windy areas, the designing and building of windmills was prevalent in Iran since 2 thousand years BC.

The implemented studies and and calculation in the filed of estimation of wind energy potential in Iran showed that the nominal capacity sites is about 6500 MW in considering to the overall efficiency of 33 percent in 26 regions of the country and this value is about one-sixth of the country's total nominal capacity of power plants [6].

The voltage control has been always one of the most important parameter of power quality in power system, in the meantime, the wind plants, having significantly reducing voltage profile in most of the time a day cuased of using induction generators and sensitivities of the plants [7].

It should be noted that according to existence statistics, the Manjil and Binalood has same problem, thus the occurred voltage changes must be quickly controlled

[8]. For this purpose, Stability Control systems of power and voltage stabilization are a remarkable significance issue for a wind farm. There are many methods for designing and stable control in nonlinear systems [9].

Ensuring the efficiency and stability, nevertheless simultaneously estimated in non-linear systems just in several methods [10]. Dynamic programming, in computer and mathematics science, is an efficient method to solve search and optimization problems using two characteristics overlapping sub-problems and optimal infrastructure [11]. The mathematician has introduced this method named Richard Bellman in 1953. Contrary to linear programming, there is no Standard framework for formulating dynamic programming problems [12].

In fact, whatever dynamic program deos is the presentation the general approach to solve this kind of problem. In any case, it should be detailed a special mathematical equations and relations that are adapted to the conditions that issue. Dynamic programming has three main characristics including principle of optimality, the optimization and overlapping sub-problems [13].

The dynamic programming technique, an array often used for storing results in order to re-use and the sub-problems solved as a part to total. Use the following procedure means that problem must be broken to smaller subproblem and find optimal respond for any of these sub-problems and earn optimal solution of general problem from gathering together the minor optimal response [14]. When a problem has an overlapping sub-problem, we have characteristic of overlapping sub-problems, if it can break the problem into smaller sub-problems, each one of response, used of multiple times during the resolution process. Dynamic programming helps not tolerating each of these responses only once calculated for solution process regarding to costs duplication. The differential active and reactive power control techniques of double-fed induction generator in [15] evaluated to control wind turbin DFIG (WT). A control technique such as proportional integral control (PI) requires a wind farm and power system with accurate modeling. Therefore, this method requires a large number of optimized parameters. Many done studies of PI controller parameters with linearing approximation set by using different optimization methods. The intelligent control strategies, such as fuzzy logic control DFIG, successfully applied in different applications. In [16], neuro-fuzzy vector control performed in a laboratory on the DFIG. In [17], fuzzy logic

control evaluated for initial frequency and active power control of wind farms. In [18], a method for designing adaptive maximum power point tracking system, suggested and evaluated by tracking fuzzy for variable speed wind generators. After more than twenty years of studies done in intelligent control of power systems, advanced control techniques, including adaptive dynamic programming (ADP) has shown that the power system has many advantages for control problems [19-20]. In this study, adaptive dynamic programming discussed for stability Control Power Systems and voltage stability in a wind farm. It should be noted present that in this study, the ability of MATLAB software will be used.

## 2. System Configuration and Modeling

Among the many existing technologies, the latest research results of both power and set of Computational Intelligence (CI) have shown that CI research can provide a key technical innovation for a solution of this challenging problem. As a result, here, representing exploration target dynamic programming (GrHDP) with the objective is attitude that applied to improve transient stability of power systems with wind penetration under fault conditions. The double-fed induction generator (DFIG) and power generators are widely used in wind power generating system [1]. Using the results [27] and [28], in this case, stability control of power system, proposed for a wind farm based on GrHDP. Introducing a new reference network, in this regard, provides a signal internal to examine critical network, our design of GrHDP show the aim that can provide control target compared to traditional design. In this case, the aim of studying is a wind farm reactive power control to improve system dynamics during and after network error, ie, reducing withdrawal swing limitation and increasing damping system.

## 3. Overview of the System Configuration

Fig. 1 shows the revised four-machine two-area system based on the classic model. This yardstick power system has been first surveyed in [10] to study the wind turbine with different controllers, such as the optimized PI controller or the nonlinear controller, to improve the transient stability performance of the power system. The system is divided into two areas, in each of which there are two machines. In [10], the four-machine two-area system is modified by replacing generator 3 (G3) with a DFIG-based wind farm. In this paper, instead of replacing G3 with a wind farm, the generator 4 (G4) is replaced with a DFIG-

based wind farm and a STATCOM. The parameters of the yardstick system and the power current can be referenced in [10].

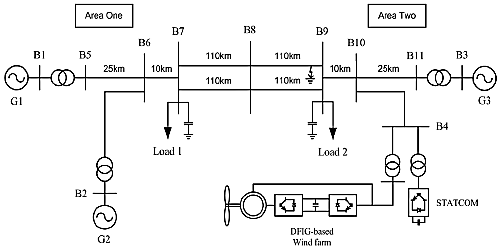


**Fig 1.** The system single-line diagram benchmark power system that includes a DFIG-based wind farm and a STATCOM.

3.1. DFIG Wind Turbine System Model

Fig. 2 explains the wind turbine model studied in this paper [4], [5]. In this system, the WT is associated with the DFIG through a drive train system, which consists of a low and a highspeed shaft with a gearbox in between. The WT with DFIG system is an induction type generator in which the stator windings are directly connected to the three-phase grid, and the rotor windings are fed through three-phase back-to-back insulated-gate bipolar transistor (IGBT) based -pulse width modulation (PWM) converters. The back-to-back PWM converter consists of a rotor-side converter (RSC), a grid-side converter (GSC) and a dc-link capacitor. Their controllers include three parts: a RSC controller, a GSC controller, and a wind turbine controller. Generally, talking, the objectives of these controllers are to maximize power production while maintaining the desired rotor speed and voltage [5]. Specifically, the WT controller controls the pitch angle of the wind turbine and the reference rotor speed to the RSC and GSC controller. Two control mechanisms are used: 1) power optimization mechanism with sub-synchronous speed; and 2) power limitation mechanism with super-synchronous speed. The RSC and GSC controller are to control the active and reactive power of the DFIG by using vector control technique.

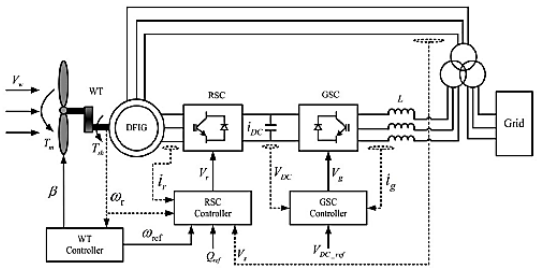


**Fig 2.** Schematic diagram of DFIG wind turbine system [4], [5]

3.2. Model of Drive Train:

The drive train system consists of a turbine, a low and a highspeed shaft, and a gearbox. A two-mass model can represent this system as follows [11]:

$$2H_t \frac{d\omega}{dt} = T_m - T_{sh} \quad (1)$$

$$\frac{d\theta_{tw}}{dt} = \omega_t - \omega_r = \omega_t - (1 - s_r)\omega_S \quad (2)$$

$$2H_g \frac{ds_r}{dt} = -T_{em} - T_{sh} \quad (3)$$

$$T_{sh} = K_{sh}\theta_{tw} + D_{sh} \frac{d\theta_{tw}}{dt} \quad (4)$$

$H_t$ : The inertia constants of the turbine; $H_g$ : The inertia constants of the generator; $\Omega_t$ : The WT angle speed; $\omega_r$ : The generator rotor angle speed; $\theta_{t\omega}$ : The shaft twist angle; $K_{sh}$ : The shaft stiffness coefficient $D_{sh}$ : The damping coefficient; $T_{sh}$ : The shaft torque; $T_m$ : The wind torque; $T_{em}$ : The electromagnetic torque.

3.3. Model of Rotor Side Controller

The RSC controller aims to control the DFIG output active power for tracking the input of the WT torque, and to maintain the terminal voltage in control setting [11]. As we mentioned before, the vector control strategy used for the active power and reactive power control of the WT with DFIG system. In order to decouple the electromagnetic torque and the rotor excitation current, the induction generator is controlled in the stator-flux-oriented reference frame, which is synchronously rotating, with its d axis oriented along the stator-flux vector position [2], [4]. Thus, for the RSC, the active power and voltage are controlled independently via $v_{qr}$ and $v_{dr}$, respectively. The voltage control achieved by controlling the reactive power is to keep it within the desired range. Fig. 3 is the overall vector control scheme of the RSC. The rotor speed $w_r$ and $Q_s$ are the measured system active power and reactive power, respectively. They are compared with the desired active power and reactive power to generate the reference signals $i_{qr\_ref}$ and $i_{dr\_ref}$. The actual d − q current signals $i_{qr}$ and $i_{dr}$ are then compared with these reference signals to generate the error signals, which are passed through two PI controllers to form the voltage signal references $v*qr$ and $v*dr$, respectively.

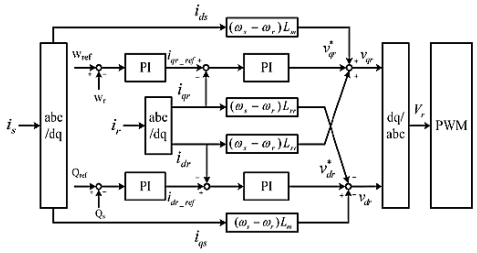


**Fig 3.** Schematic diagram of the control rotor-side

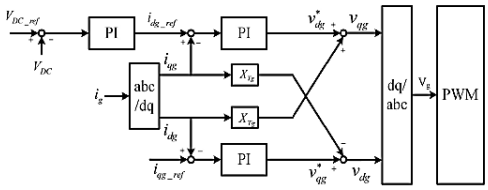


**Fig 4**. Schematic diagram of the control grid side

The two voltage signals $v*qr$ and $v*dr$ are compensated by the conforming cross-coupling terms to form the voltage signals $v_{qr}$ and $v_{dr}$. After reference frame transformation, control signal $V_r$ is then used by the PWM module to generate the IGBT gate control signals to drive the RSC.

3.4. Model of Grid Side Controller

The GSC, as showed in Fig. 4, aims to maintain the dc-link voltage, and to control the terminal reactive power [11]. In order to obtain independent control of the active and reactive power flowing between the grid and the grid side converter, the converter control operates in the grid-voltage oriented reference frame, which is synchronously rotating, with its d axis oriented along the gridvoltage vector position [2], [4]. Thus, the dc-link voltage and reactive power are controlled independently via $v_{dg}$ and $v_{qg}$, respectively. The actual signal of the dc-link voltage $V_{DC}$ compared with its command value $V_{DC\_ref}$ to form the error signal, which is passed through the PI controller to generate the reference signal $i_{dg\_ref}$. Then this reference signal $i_{dg\_ref}$ and another corresponding reference signal $i_{qg\_ref}$ are compared with the actual signals $i_{qg}$ and $i_{dg}$, respectively. These error signals are then passed through two PI controllers to form the voltage signal references $v*dg$ and $v*qg$, respectively. The two voltage signals $v*dg$ and $v*qg$ are compensated by the corresponding cross-coupling terms to form the voltage signals $v*dg$ and $v*qg$. After reference frame transformation, control signal $V_g$ is then used by the PWM module to generate the IGBT gate control signals to drive the GSC.

3.5. STATCOM Model

The STATCOM and its controllers are shown in Fig. 5. It is a shunt device of the flexible alternating current transmission system (FACTS) family using power electronics to control power flow and improve transient stability of power grids [6]–[8].

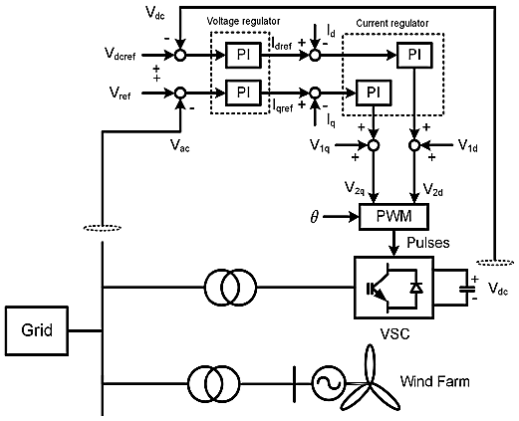


**Fig. 5.** Schematic diagram of STATCOM control

The STATCOM regulates voltage at its terminal by controlling the amount reactive power injected into or absorbed from the power grid, which depends on the system voltage. The STATCOM modeling based on IGBT, but as details of the inverter and harmonics are not represented, it can also be used to model a gate-turn-off thyristor (GTO) based STATCOM in transient stability studies. In the controller design, an outer regulation loop consists of an ac voltage regulator and a dc voltage regulator, while an inner regulation loop consists of a current regulator. The current regulator is

assisted by a feed forward type regulator which predicts $V_{2d}$ and $V_{2q}$ from the measurementsthe transformer $V_{1q}$ and $V_{1d}$ leakage reactance [6]. During normal conditions, both active and reactive power flow to/from the STATCOM are very low. Active power demand is only the losses within the STATCOM, and reactive power demand is within the difference between neighbor steps of switchable ac filters [29]. When the system is under fault conditions, both STATCOM active and reactive power demands are significantly increased. Because of the high cost, the rating of the STATCOM should be carefully addressed in practical applications. The minimal capacity of STATCOM should be chosen above the given curve for particular value of communication delay and a detailed engineering study of the STATCOM sizing is presented in [29].

3.6. GrHDP-Based controller design

The GrHDP architecture includes three parts: an action network, a critic network, and a reference network [27], [28]. The action network produces control signal $u(t)$ according to a learning policy represented by approximating network, while the reference network provides the internal reinforcement signal (internal goal/reward representation) $s(t)$, to interact with the critic network to approximate the cost and reward function J by minimizing the Bellman function as follows:

$$J^*(x(t))=\min_{u(t)}\left\{Ux(t),u(t)+\gamma * J^*(x(t+1))\right\} \quad (5)$$

Where $x(t)$ the state vector of the system, U is the utility function and γ is a discount factor. These three parts are usually implemented by using neural networks because of their universal approximation capability and the associated backpropagation learning algorithm. During the on-line learning, the controller is "naive" when it starts to control, namely, the action network, critic network and reference network are both randomly initialized in their weights. Once a system state is observed, an action will be subsequently produced based on the parameters in the action network. Indirectly principle is the ultimate desirable goal contact-error-propagation in the implementation of operational network, denoted by $U_c$, and the approximate J functions from the critic network. Based on the instant reinforcement signal and internal reinforcement signal, the controller will learn to accomplish the control goal. The error functions used to update the parameters in the action network, critic network and reference network are as follows:

$$\begin{cases} e_a(t) = J(t) - U_c(t) & E_a(t) = \frac{1}{2}e_a^2(t) \\ e_f(t) = \alpha J(t) - [J(t-1) - r(t)]; & E_f(t) = \frac{1}{2}e_f^2(t) \\ e_c(t) = \alpha J(t) - [J(t-1) - s(t)]; & E_c(t) = \frac{1}{2}e_c^2(t) \end{cases} \quad (6)$$

The chain back-propagation rule is employed to train and adapt the parameters in the three neural networks as follows

where ωa, ωf and ωc are the weights of action network, reference network and critic network, respectively. Fig. 6 shows the DFIG wind turbine system and STATCOM with the proposed GrHDP controller. The upper area denotes the plant to be controlled by the GrHDP controller. The system state $X(t)$ is measured as the GrHDP controller input signal. Then the output signal or action signal $u(t)$ produced by the controller as supplementary control signals send to the RSC controller and the STATCOM controller.

3.7. Input, Output, and Reinforcement Signal Design

As an on-line controller with instant learning from the environment, the performance of the GrHDP controller is mainly, depend on the design of the input, output and reinforcement signal. Figs. 7 and 8 show active power from area one to area two and active power of the wind farm after a threephase ground-fault applied at 5 s, respectively. The applied fault causes oscillation of the active power of the whole system. After the fault, the active power of the wind farm (Fig. 8) damps within about 1 s, but the transferred active power oscillation (Fig. 7) lasts much longer, i.e., 3 s. The principle of the GrHDP controller for the benchmark power system is discussed as follows. The supplementary control signals $\Delta V_{ref}$ and $\Delta Q_{ref}$ will change with the system states When the system is under error conditions. With appropriate adjustment, the controller can reduce the level of voltage dips of the wind farm as well as the PCC point, and improve the transient stability of the whole system after the fault. Because of the direct coupling between the voltage and the reactive power, it is straightforward to use the voltage deviation $\Delta V_{wind}$ as the first of the three input signals to the controller. The active power deviation of the wind farm $\Delta V_{wind}$ also considered as the second input signal to the GrHDP controller to provide additional information, thus providing better control performance [18]. As we mentioned before, since the dynamics of the system last longer than (that of) the wind farm, therefore the deviation of the transferred active power from area one to area two is also considered as the third and last input signal. The design of the reinforcement signal $r(t)$ in (9) based on the external environment, which represented by the wind farm and the

system oscillation. The control of the wind farm and the STATCOM is coordinated, to some extent, as the system states combined in one index as indicated in the designed $r(t)$.

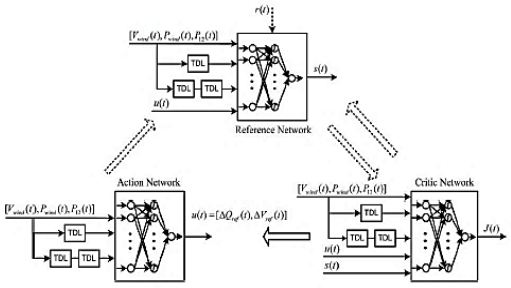


**Fig 6.** Implementation and cooperative learning of the GrHDP controlle

3.8. Implementation of the Action, Critic, and Reference Network

Fig. 9 shows the implementation of the action, critic, and reference network. We can observe that, the $s(t)$ signal provides an important link between the reference network and the critic network, which makes the chain back-propagation able to adjust the parameters in the reference network and critic network. Furthermore, compared with the classical ADP, the $s(t)$ signal is served as an adaptive reinforcement signal $r(t)$ to the critical network. In this way, multiple-level internal goals are formed by the GrHDP to fulfill the long-term final goal. A cooperative learning strategy is used which involves more interactions between the reference network and the critic network [27]. In this learning strategy, at each epoch of the parameter-tuning, one can first adapt the reference network weights based on the primary reinforcement signal $r(t)$ through back-propagation. Then the reference network will output the secondary reinforcement signal $s(t)$, which will be used to tune the weights in the critic network through back-propagation. Once the weights in critic network are tuned in this epoch, the critic network will provide a new $J(t)$ estimation, which in turn can be used to adapt the weights in reference network in the next epoch.

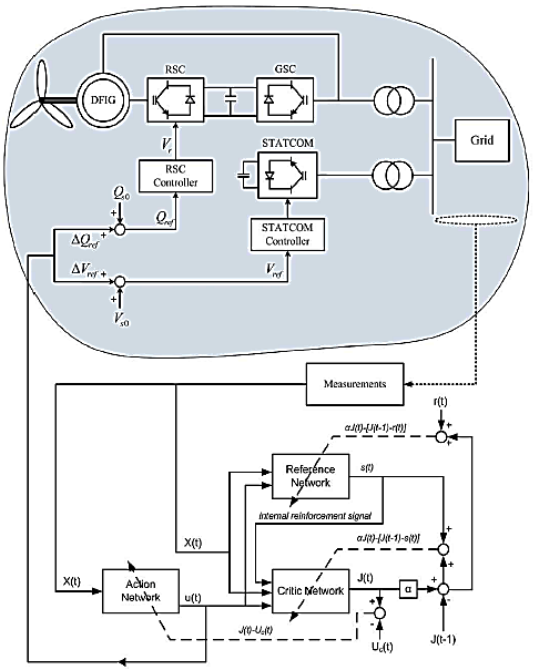


**Fig. 7.** Schematic diagram of the GrHDP controller with the plant

$$\begin{cases} \dfrac{\partial E_a(t)}{\partial \omega_a(t)} = \dfrac{\partial E_g(t)}{\partial J(t)} \dfrac{\partial J(t)}{\partial u(t)} \dfrac{\partial u(t)}{\partial \omega_a(t)} \\ \dfrac{\partial E_f(t)}{\partial \omega_f(t)} = \dfrac{\partial E_f(t)}{\partial J(t)} \dfrac{\partial J(t)}{\partial s(t)} \dfrac{\partial s(t)}{\partial \omega_f(t)} \\ \dfrac{\partial E_c(t)}{\partial \omega_c(t)} = \dfrac{\partial E_c(t)}{\partial J(t)} \dfrac{\partial J(t)}{\partial \omega_c(t)} \end{cases} \quad \textbf{(7)}$$

Therefore, it is reasonable to consider the system dynamics (oscillation between the two areas) into the input, output and reinforcement signal design. The input signal of the controller designed as follows:

$$\begin{cases} \Delta V_{wind}(t), \Delta V_{wind}(t-1), \Delta V_{wind}(t-2) \\ \Delta P_{wind}(t), \Delta P_{wind}(t-1), \Delta P_{wind}(t-2) \\ \Delta P_{12}(t), \Delta P_{12}(t-1), \Delta P_{12}(t-2) \end{cases} \quad (8)$$

Where $\Delta V_{wind}$ is the voltage deviation of the wind farm $\Delta P_{wind}$ , is the active power deviation of the wind farm and $\Delta P_{12}$ is the deviation of transferred active power from area one to area two.

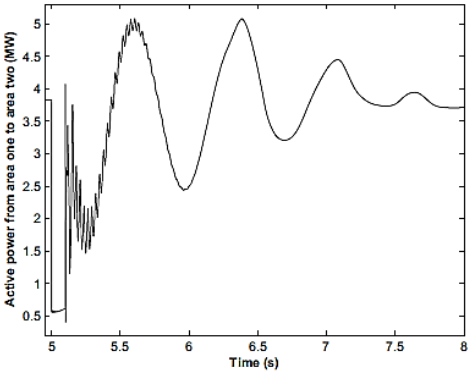


**Fig. 8**. Active power from area one to area two after system fault

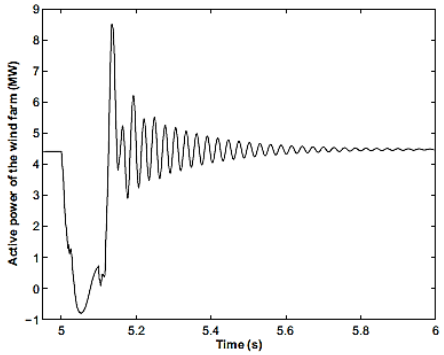


**Fig. 9.** Active power of the wind farm after system faul

The output signals of the controller are $\Delta Q_{ref}(t)$ and $\Delta V_{ref}(t)$, which are send to the wind farm and the STATCOM as supplementary control signals. The reinforcement signal of the controller designed as follows

$$\begin{aligned} r(t) = & -\Delta V_{wind}^2(t) - 0.5 * \Delta V_{wind}^2(t-1) \\ & -0.1*\Delta V_{wind}^2(t-2) - \Delta V_{wind}^2(t) \\ & -0.5*\Delta P_{wind}^2(t-1) - 0.1*\Delta P_{wind}^2(t-2) \\ & -\Delta P_{12}^2(t) - 0.5*\Delta P_{12}^2(t-1) - 0.1*\Delta P_{12}^2(t-2) \\ & -3 * \Delta \omega_{12}^2(t) \end{aligned} \quad (9)$$

## 4. Result and Discussion

The proposed GrHDP controller and the benchmark power system are implemented in MATLAB/Simulink environment. To make comprehensive comparison, the traditional ADP (i.e., direct HDP) algorithm in [21] also applied to control the DFIG-based wind farm and the STATCOM, presented two scenarios to verify the effectiveness of the proposed controller. During the simulation, all the synchronous

machines are equipped with automatic voltage regulator (AVR), speed regulator, and PSS. The proposed GrHDP controller provides supplementary control signals to the regular PI controllers in DFIG and STATCOM.

4.1. Scenario I

In this scenario, the wind speed kept constant at 11 m/s. The steady state commands of DFIG and STATCOM are set as $Q_{s0}=0$ and $V_{s0}=1$, respectively. A three-phase ground-fault with ground resistance of $0.01\Omega$ applied at B9 at $t=5s$, where the fault is cleared at $t=5.1s$ without tripping the line. The simulations are carried out to compare the transient dynamics of the wind farm and the system using the GrHDP controller, direct HDP controller and PI controller. The Fig. 10-15 shows the simulation results of various variables of this benchmark under the situation of with GrHDP controller, direct HDP controller and PI controller.

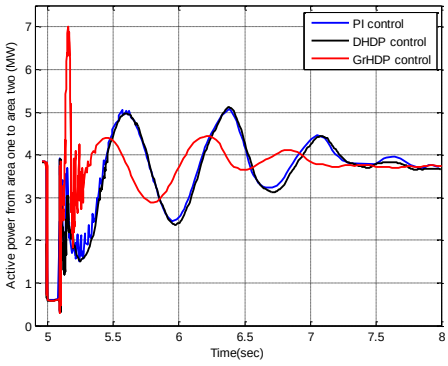


**Fig.10**. Active power graph from area one to area two

Specifically, as shown in Fig. 10 you can see the active power transferred from area to area two shows that first, we see fluctuations in active power and and then as shown in Figure 11, these fluctuations gradually dropped to zero. Figure 11 shows the difference of rotor angle between two areas shows the same behavior in Fig. 10. It can be observed that the transient stability of wind farm and system is improved by using the controller HDP and HDP direct control.

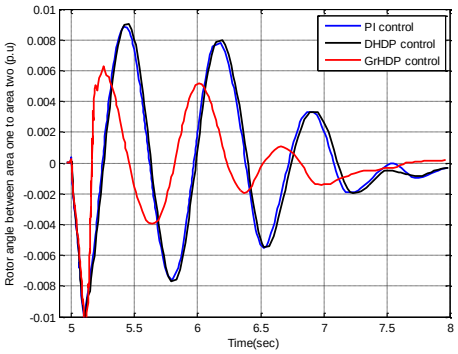


**Fig 11.** Rotor angle of a are one to the are two

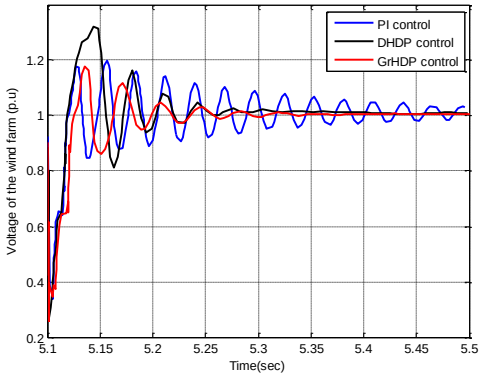


**Fig 12.** wind farm Voltage

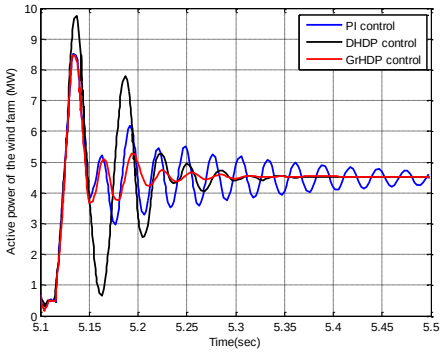


**Fig 13.** Active power of wind farm

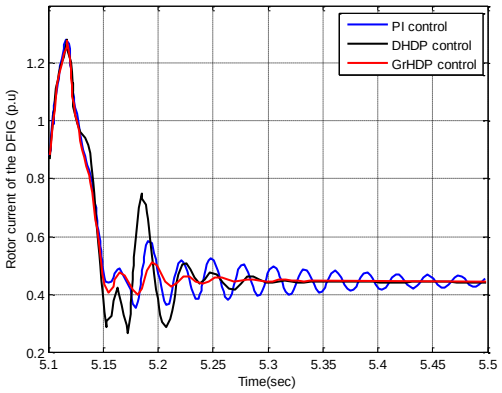


**Fig 14.** DFIG rotor current

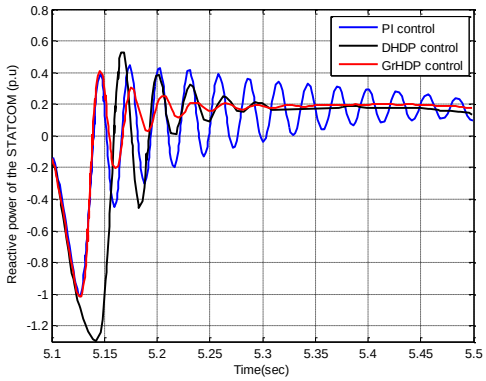


**Fig 15**. STATCOM reactive power

In Fig. 12 and Fig. 10, shows wind farm voltage and wind farm power respectively. In Figure 12 voltage range of 2.0 to 4.1 is intended to limit the scope of changes in parameters to reach their highest after going few times lay down to 1 and also active power range has been reached between 4 to 5 MW. It can be observed that the transient stability of wind farm and system is improved by using the controller HDP and HDP direct control. In Fig. 14 and Fig. 15, shows DFIG rotor current and reactive power STATCOM. As can be seen in both the 13 and 14, similar to previous Figs, range of parameters at first reach to their highest limit after going few times lay down. It can be observed that the transient stability of wind farm and system is improved by using the controller HDP and HDP direct control. In addition, the control effect of the proposed HDP controller is much better than HDP direct control.

4.2. Scenario II

To verify the robustness of the proposed GrHDP controller, the configuration of the benchmark power system in Fig. 1 is modified. Specifically, the capacity of G1, G2, G3, and G4 are increased from 9 to 400 MW. Meanwhile, we assume one of the transmission lines between these two areas (the lower one in Fig. 1) is out-of-service, which represents the system is much more vulnerable than the original one. The speed of the wind in the DFIG-based wind farm is kept constant at 11 m/s. The steady state commands of DFIG and STATCOM are the same as before with $Q_{s0} = 0$ and $V_{s0} = 1$,

respectively. A three-phase ground-fault with ground resistance of $0.01\Omega$ is applied near B8 at $t = 1.5s$, and the fault is cleared at $t = 5.1s$ without tripping the line. In Fig 16-21 demonstrates the simulation results of various variables of this benchmark under the situation of with GrHDP controller, direct HDP controller and PI controller.

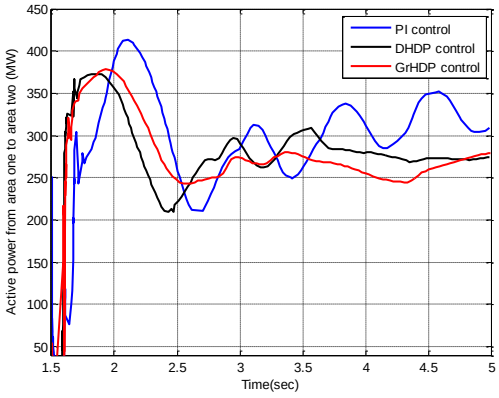


**Fig 16**. Active power from area one to area two

As can be seen in Fig 16 Active power is transferred from area one to area two, having a range between 50 to 400 MW and created the early second wave of extremely non-stable range that sit on a certain range of these waves and as much as possible, reducing the amount of error. This mode is similar to Fig 17 shows the rotor angle difference between the two areas.

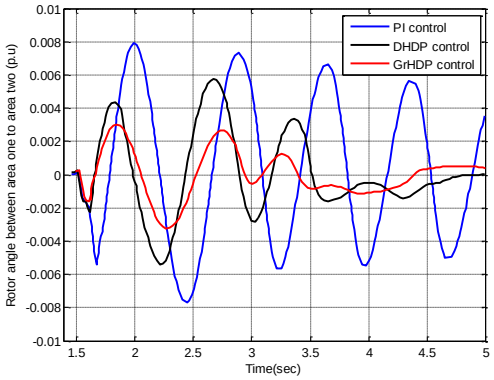


**Fig 17.** Rotor angle between a area one and the area two

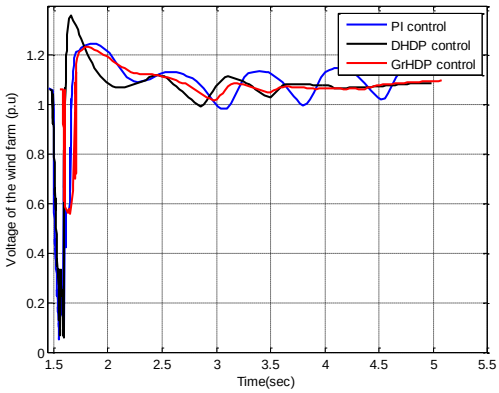


**Fig 18.** Wind Farm Voltage

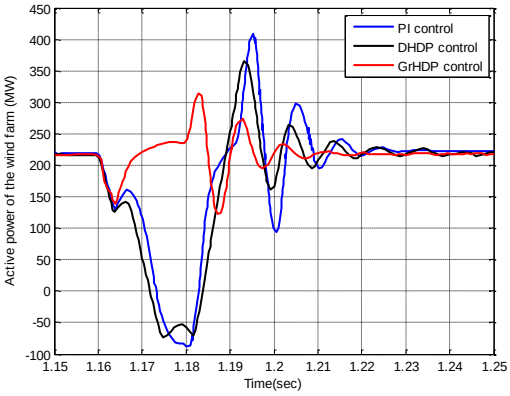


**Fig 19**. Active power of wind farm

Figure 18 and 19 shows voltage wind farm and active power wind farm that the

variation range shows in primary seconds creating of range wave would be appeared highly non-stable mode and this result can be seen that we initially have severe computing error, the system has been stable after period of time and reduce errors as much as possible.

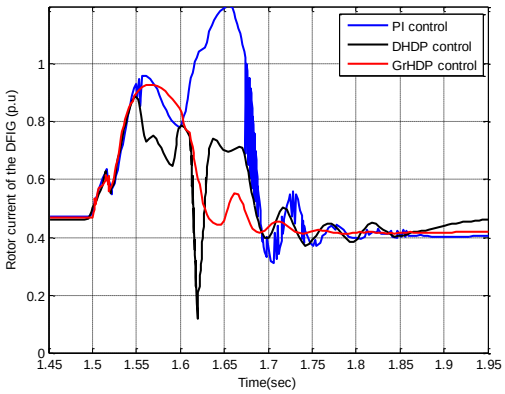


**Fig 20.** DFIG rotor current

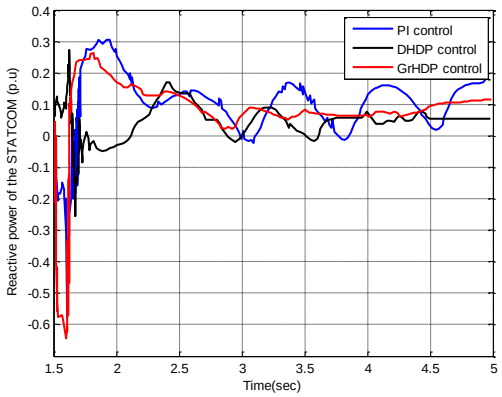


**Fig 21.** STATCOM reactive power

In Fig. 20 and Fig. 21 shows, rottor current, STOTCOM reactive respectively, and having great fluctuations in some of the time similar to previous Figs that shows Severe error moment at the beginning of swinging what is reducing error after period of time. These results show that the system is still stable while using the controller HDP and HDP direct control, and transient dynamics of the wind farm and system are improved. By controlling the GDP, LVRT capability wind farm significantly are improved compared to the other two methods. In addition, these results suggest that strong ability to optimize the control of the proposed GrHDP would be such as when system operation conditions or configuration changes, GrHDP control indicates that the control performance is satisfied.

4.3. The analysis of control results

*S*ingle-phase *s*urface error *is* 220 kV at 30 seconds *near to* bus, *e*rror *f*or 150 milliseconds lasted by disconnecting a tra*nsmission line.* Evolution weighs carried out about connecting the *input units to the hidden units i*ndicates the GDP Control learning process.

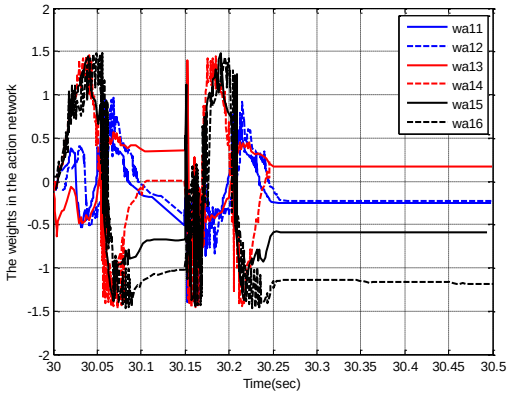


**Fig 22.** Learning process has been represented by the evolution of the individual weight connecting the input units to one of the hidden units in the action network.

Directly, we can see that all the weight converged after 3/30 seconds. Note that the timing errors (30 to 15/30 seconds) and time of error (15/30 to 30/30 seconds) are two steps away from the controls. These two stages-times error shows the evolution of weight in addition to two learning process. At each stage, dramatically weight originally comprised much tension and convergence occurs after matching. This learning process is compatible with complementary output of control signal curve, as shown in Figure 23.

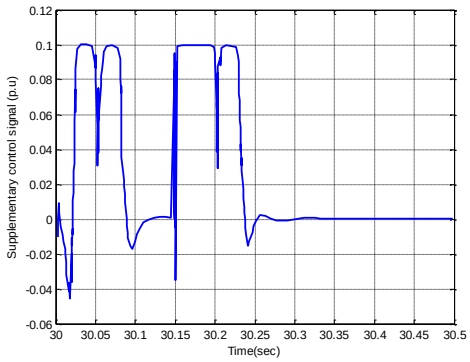


**Fig 23.** Additional control signals generated by the network operation

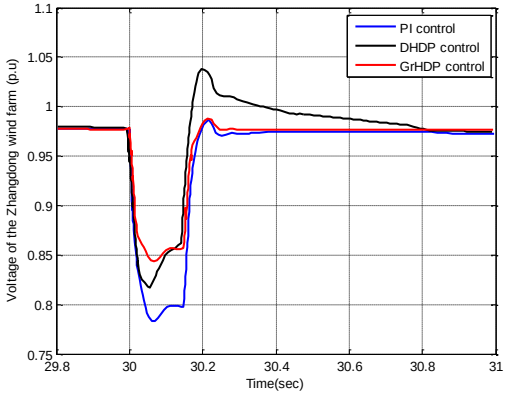


**Fig. 24.** Performance of wind farm voltage after training

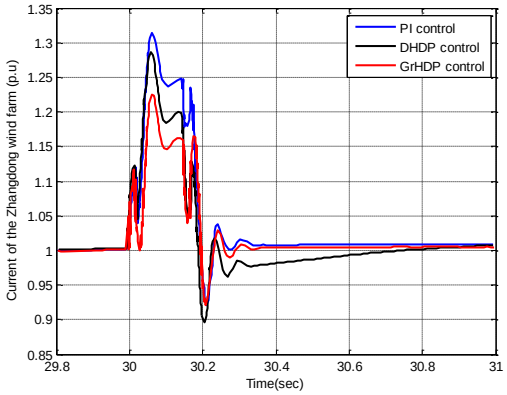


Fig. 25. Performance of wind farm current after training

After finishing the learning process, the voltage and current of wind farm at Bus15 are improved by the proposed GrHDP controller, compared with the performance of PI controller and direct HDP controller, as shown in Figs. 24 and 25.

## Conclusion

In this paper, an adaptive controller based on GrHDP for DFIG-based wind farm is proposed. We presented the detailed control architecture, and tested the approach on two cases, i.e., a revised four-machine two-area system with wind penetration and a practical size power system with wind farm. Comparative studies of our method with existing approaches were also presented in this paper. Simulation results demonstrated that with the proposed GrHDP controller, the transient stability of the wind farm under grid fault conditions could be improved. LVRT capability of the wind farm and the system could also be enhanced. The characteristics of the online GrHDP approach are similar to other ADP approaches where the approximation of J is not based on the pretraining data set but on the error functions from interaction with the environment (power plant in this paper) in each time step. However, the formulated temporal difference (TD) learning algorithm in the three networks in GrHDP guaranteed that the expected values of the prediction converge to the correct values, give appropriate samples, and learning iterations. There are several interesting directions for future research along this topic. For instance, the supplementary control ability of GrHDP for high-voltage direct current and various FACTS devices could be developed to construct wide-area damping control systems. Since the GrHDP demonstrates robust learning and universal control characteristics, it could also be utilized for stability enhancement of large-scale interconnected power systems.

## Refeences

[1] A. Grauers, “Efficiency of three wind energy generator system,” IEEE Trans. Energy Convers., vol. 11, no. 3, pp. 650–657, Sep. 1996.

[2] R. Pena, J. C. Clear, and G. M. Asher, “Doubly fed induction generator using back-to-back PWM converters and its application to variable-speed wind energy generation,” IEE Proc. Elect. Power Appl., vol. 143, no. 3, pp. 231–241, May 1996.

[3] E. Vittal, M. O’Malley, and A. Keane, “Rotor angle stability with high penetrations of wind generation,” IEEE Trans. Power Syst., vol. 27, no. 1, pp. 353–362, Feb. 2012.

[4] L. Yang, Z. Xu, J. Ostergaard, Z. Y. Dong, and K. P. Wong, “Advanced control strategy of DFIG wind turbines for power system fault ride through,” IEEE Trans. Power Syst., vol. 27, no. 2, pp. 713–722, May 2012.

[5] A. D. Hansen, P. Sørensen, F. Iov, and F. Blaabjerg, “Control of variable speed wind turbines with doubly-fed induction generators,” Wind Eng., vol. 28, no. 4, pp. 411–434, 2004.

[6] N. G. Hingorani and L. Gyugyi, Understanding FACTS: Concepts and Technology of Flexible AC Transmission Systems. Hoboken, NJ USA: Wiley, 2000.

[7] M. S. El Moursi, B. Bak-Jensen, and M. H. Abdel-Rahman, “Coordinated voltage control

scheme for SEIG-based wind park utilizing substation STATCOM and ULTC transformer," IEEE Trans. Sustain. Energy, vol. 2, no. 3, pp. 246–255, Jul. 2011.

[8] C. Han et al., "STATCOM impact study on the integration of a large wind farm into a weak loop power system," IEEE Trans. Energy Convers., vol. 23, no. 1, pp. 226–233, Mar. 2008.

[9] M. Yamamoto and O. Motoyoshi, "Active and reactive power control for doubly-fed wound rotor induction generator," IEEE Trans. Power Electron., vol. 6, no. 4, pp. 624–629, Oct. 1991.

[10] F. Wu, X. P. Zhang, P. Ju, and M. J. H. Sterling, "Decentralized nonlinear control of wind turbine with doubly fed induction generator," IEEE Trans. Power Syst., vol. 23, no. 2, pp. 613–621, May 2008.

[11] F. Wu, X. P. Zhang, K. Godferey, and P. Ju, "Small signal stability analysis and optimal control of a wind turbine with doubly fed induction generator," IET Gen. Transmiss. Distrib., vol. 1, no. 5, pp. 751–760, Sep. 2007.

[12] Y. Tang, P. Ju, H. He, C. Qin, and F. Wu, "Optimized control of DFIGbased wind generation using sensitivity analysis and particle swarm optimization," IEEE Trans. Smart Grid, vol. 4, no. 1, pp. 509–520, Mar. 2013.

[13] H. M. Jabr, D. Lu, and N. C. Kar, "Design and implementation of neurofuzzy vector control for wind-driven doubly-fed induction generator," IEEE Trans. Sustain. Energy, vol. 2, no. 4, pp. 404–413, Oct. 2011.

[14] A. Kusiak and Z. J. Zhang, "Adaptive control of a wind turbine with data mining and swarm intelligence," IEEE Trans. Sustain. Energy, vol. 2, no. 1, pp. 28–36, Jan. 2011.

[15] V. Galdi, A. Piccolo, and P. Siano, "Designing an adaptive fuzzy controller for maximum wind energy extraction," IEEE Trans. Energy Convers., vol. 23, no. 2, pp. 559–569, Jun. 2008.

[16] P. J. Werbos, "Computational intelligence for the smart grid-history, challenges, and opportunities," IEEE Comput. Intell. Mag., vol. 6, no. 3, pp. 14–21, Aug. 2011.

[17] G. K. Venayagamoorthy, "Dynamic, stochastic, computational, and scalable technologies for smart grids," IEEE Comput. Intell. Mag., vol. 6, no. 3, pp. 22–35, Aug. 2011.

[18] W. Qiao, R. G. Harley, and G. K. Venayagamoorthy, "Coordinated reactive power control of a large wind farm and a STATCOM using heuristic dynamic programming," IEEE Trans. Energy Convers., vol. 24, no. 2, pp. 493–503, Jun. 2009.

[19] J. Liang, G. K. Venayagamoorthy, and R. G. Harley, "Wide-area measurement based dynamic stochastic optimal power flow control for smart grids with high variability and uncertainty," IEEE Trans. Smart Grid, vol. 3, no. 1, pp. 59–69, Mar. 2012.

[20] D. Molina, G. K. Venayagamoorthy, J. Liang, and R. G. Harley, "Intelligent local area signals based damping of power system oscillations using virtual generators and approximate dynamic programming," IEEE Trans. Smart Grid, vol. 4, no. 1, pp. 498–508, Mar. 2013.

[21] J. Si and Y. T. Wang, "Online learning control by association and reinforcement,"

IEEE Trans. Neural Netw., vol. 12, no. 2, pp. 264–276, Mar. 2001.

[22] C. Lu, J. Si, and X. R. Xie, “Direct heuristic dynamic programming for damping oscillations in a large power system,” IEEE Trans. Syst., Man, Cybern. B, Cybern., vol. 38, no. 4, pp. 1008–1013, Aug. 2008.

[23] Y. Tang, H. He, Z. Ni, J. Wen, and X. Sui, “Reactive power control of grid-connected wind farm based on adaptive dynamic programming,” Neurocomputing, vol. 125, pp. 125–133, Feb. 2014.

[24] Y. Tang, H. He, and J.Wen, “Adaptive control for an HVDC transmission link with FACTS and a wind farm,” in Proc. IEEE PES Innov. Smart Grid Technol. (ISGT), Washington, DC, USA, Feb. 2013, pp. 1–6.

[25] Y. Tang, H. He, and J. Wen, “Comparative study between HDP and PSS on DFIG damping control,” in Proc. IEEE Symp. Comput. Intell. Appl. Smart Grid (CIASG), Singapore, Apr. 2013, pp. 59–65.

[26] X. Sui, Y. Tang, H. He, and J. Wen, “Energy-storage-based lowfrequency oscillation damping control using particle swarm optimization and heuristic dynamic programming,” IEEE Trans. Power Syst., vol. 29, no. 5, pp. 2539–2548, Sep. 2014.

[27] H. He, Z. Ni, and J. Fu, “A three-network architecture for on-line learning and optimization based on adaptive dynamic programming,” Neurocomputing, vol. 78, no. 1, pp. 3–13, 2012.

[28] Z. Ni, H. He, and J. Wen, “Adaptive learning in tracking control based on the dual critic network design,” IEEE Trans. Neural Netw. Learn. Syst., vol. 24, no. 6, pp. 913–928, Jun. 2013.